Viscoelastic Microbuckling of Fiber Composites

W. S. Slaughter

N. A. Fleck

Engineering Department,
Cambridge University,
Trumpington Street,
Cambridge, CB2 1PZ, England

A theoretical study is given of viscoelastic microbuckling of fiber composites. The analysis is formulated in terms of general linear viscoelastic behavior within the kink band. Material outside the kink band is assumed to behave elastically. Two specific forms of linear viscoelastic behavior are considered: a standard linear viscoelastic model and a logarithmically creeping model. Results are provided as deformation versus time histories and failure life versus applied stress. Failure is due to either the attainment of a critical failure strain in the kink band or to the intervention of a different failure mechanism such as plastic microbuckling.

Introduction

Microbuckling has been shown usually to be the dominant mechanism of compressive failure of aligned fiber composite materials (Argon, 1972; Budiansky and Fleck, 1993). The form of microbuckling under consideration here is an event in which the composite suffers localized buckling within a kink band. In laminates this is commonly observed in plies with fiber axes that are parallel to the loading direction. Matrix cracking of off-axis plies (plies with fiber axes not in the loading direction) and inter-ply delamination may occur concurrently, but microbuckling is thought to control failure when the proportion of off-axis plies is not large (Soutis, 1991). A physical understanding of the factors which control microbuckling is therefore important in order to design fiber composites of improved compressive strength.

Several studies of time-*independent* compressive failure have been undertaken. A preliminary theoretical analysis by Rosen (1965) treated microbuckling as an elastic buckling phenomenon. Results from this analysis, however, severely overestimate the critical stresses necessary for microbuckling. Subsequent theoretical analyses which have sought to modify the Rosen model to account for this discrepancy between predicted and measured strengths (e.g., Steif, 1988) have met with limited success. More recent studies by Argon (1972) and Budiansky and Fleck (1993) have included the effects of matrix yielding, initial fiber misalignment, and fiber extensibility. In these analyses, the assumption is made that a band of misaligned fibers exists and that the composite exhibits a predilection to microbuckle uniformly within this band. These latter studies form the foundation on which the current analysis is based.

Many fiber composites are known to exhibit time-*dependent* deformation behavior. Two of the more common examples, carbon fiber-reinforced PEEK and carbon fiber-reinforced epoxy resin, have been studied at ambient temperature (Horoschenkoff et al., 1988) and at elevated temperatures (Ha et al., 1991). In this paper, a linear viscoelastic composite behavior is assumed in order to examine time-dependent microbuckling of fiber composites in compression. The solution is formulated in terms of a general relaxation function and specific results are given for a standard linear viscoelastic solid and a logarithmically creeping solid. The logarithmic creep behavior is derived from the results of Horoschenkoff et al. (1988).

The results of this study may also be applicable to woods. Many woods fail by microbuckling in the S_2 layer of the cell wall (Grossman and Wold, 1971; Dinwoodie, 1981). The cell wall is composed of over 90 percent aligned tracheids by volume, which are natural fibers, bonded together by a weaker substance consisting principally of pectopolyuronides and lignin (Mark, 1967). These tracheids can be thought of as analogous to fibers in a fiber composite and the weaker bonding material as analogous to the matrix. Wood is also known to behave viscoelastically (Mark, 1967; Dinwoodie, 1981). Thus, to a first approximation, wood may be thought of as a viscoelastic fiber composite.

Viscoelastic Microbuckling

In microbuckling of uniform, aligned fiber composites, a kink band is formed in which the composite undergoes localized catastrophic failure. This kink band is on the order of ten fiber diameters in width and is generally *not* normal to the fiber axes. A schematic of the kink band is shown in Fig. 1. The kink band is at an angle β to the transverse direction and is of width w. It is assumed that the fibers are inextensible and that deformation within the band can be represented by the change in fiber direction ϕ. It is also assumed that an initial imperfection, or misalignment, can be represented by $\bar{\phi}$. Variations along the kink band are ignored. Let two cartesian coordinate systems, $(\underline{e}_1,\underline{e}_2)$ and $(\underline{\epsilon}_1,\underline{\epsilon}_2)$, aligned with the fiber direction outside and inside the kink, respectively, be defined

Contributed by the Applied Mechanics Division of THE AMERICAN SOCIETY OF MECHANICAL ENGINEERS for presentation at the ASME Winter Annual Meeting, New Orleans, LA, Nov. 28–Dec. 3, 1993.

Discussion on this paper should be addressed to the Technical Editor, Professor Lewis T. Wheeler, Department of Mechanical Engineering, University of Houston, Houston, TX 77204-4792, and will be accepted until four months after final publication of the paper itself in the ASME JOURNAL OF APPLIED MECHANICS.

Manuscript received by the ASME Applied Mechanics Division, Apr. 3, 1992; final revision, Dec. 3, 1992. Associate Technical Editor: G. J. Dvorak.

Paper No. 93-WA/APM-16.

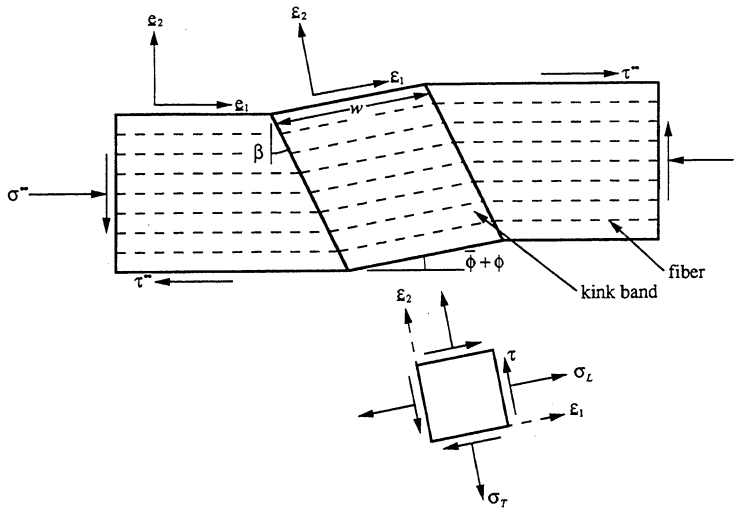

Fig. 1 Kink band geometry and notation

as shown in Fig. 1. For simplicity, remote loading $\underline{\sigma}^\infty = -\sigma^\infty \underline{e}_1\underline{e}_1 + \tau^\infty(\underline{e}_1\underline{e}_2 + \underline{e}_2\underline{e}_1)$ is restricted to be proportional and prescribed by the parameter $e \equiv \tau^\infty/\sigma^\infty$. We neglect remote loading perpendicular to the fibers.

A uniform state of stress and strain, related by a linear elastic response, is assumed to exist outside the kink band. Within the kink band the stress is given by $\underline{\sigma} = \sigma_L \underline{\epsilon}_1\underline{\epsilon}_1 + \sigma_T \underline{\epsilon}_2\underline{\epsilon}_2 + \tau(\underline{\epsilon}_1\underline{\epsilon}_2 + \underline{\epsilon}_2\underline{\epsilon}_1)$ and the strain is given by $\underline{\epsilon} = e_T \underline{\epsilon}_2\underline{\epsilon}_2 + (1/2)\gamma(\underline{\epsilon}_1\underline{\epsilon}_2 + \underline{\epsilon}_2\underline{\epsilon}_1)$. Expressions for kinematic conditions and continuity of tractions across the kink band interface have been derived by Budiansky and Fleck (1993). In the $\underline{\epsilon}_2$-direction perpendicular to the kink band fibers, continuity of tractions requires

$$\sigma^\infty[\cos\beta\sin(\bar{\phi}+\phi) + e\cos(\beta+\bar{\phi}+\phi)] = \tau\cos(\beta-\bar{\phi}-\phi) + \sigma_T\sin(\beta-\bar{\phi}-\phi). \quad (1)$$

For small ϕ and $\bar{\phi}$ the approximate kinematic equations, relating strains within the kink band to ϕ, are (Budiansky and Fleck, 1993)

$$\gamma \approx \phi + \gamma^\infty = \phi + \frac{e\sigma^\infty}{G} \quad (2)$$

$$e_T \approx \phi\tan\beta \quad (3)$$

where γ^∞ is the shear strain outside the kink band and G is the composite shear modulus. The kink band angle β changes with remote shear strain γ^∞ according to

$$\tan\beta = \tan\beta_0 - \gamma^\infty$$

where β_0 is the initial value of β. For small γ^∞, $\beta \approx \beta_0$.

Within the kink band, the composite is assumed to have a linear viscoelastic response with independent transverse and shear constitutive relations; if $\lim_{t\to-\infty}\gamma(t) = \lim_{t\to-\infty} e_T(t) = 0$ then

$$\tau(t) = \int_{-\infty}^{t} K_S(t-s)\dot{\gamma}(s)ds = K_S(0)\gamma(t) + \int_{-\infty}^{t} \dot{K}_S(t-s)\gamma(s)ds \quad (4)$$

$$\sigma_T(t) = K_T(0)e_T(t) + \int_{-\infty}^{t} \dot{K}_T(t-s)e_T(s)ds \quad (5)$$

where t is time and $\dot{f}(t) \equiv \frac{d}{dt}f(t)$. $K_S(t)$ and $K_T(t)$ are the composite relaxation functions in shear and transverse straining, respectively. Substituting Eq. (2)–(5) into (1) gives

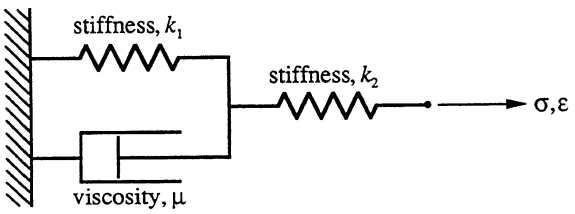

Fig. 2(*a*) Representative diagram for standard linear viscoelastic solid

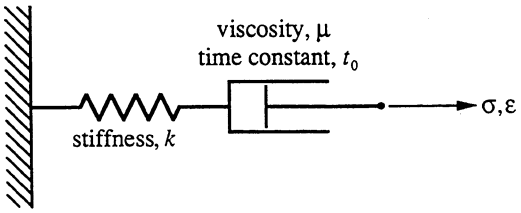

Fig. 2(*b*) Representative diagram for logarithmically creeping solid

$$\sigma^\infty[\cos\beta\sin(\bar{\phi}+\phi) + e\cos(\beta+\bar{\phi}+\phi)] - \left\{K_S(0)\left(\phi + \frac{e\sigma^\infty}{G}\right) + \int_{-\infty}^{t} \dot{K}_S(t-s)\left[\phi(s) + \frac{e\sigma^\infty(s)}{G}\right]ds\right\}\cos(\beta-\bar{\phi}-\phi) - \left\{\phi K_T(0) + \int_{-\infty}^{t} \dot{K}_T(t-s)\phi(s)ds\right\}\tan\beta\sin(\beta-\bar{\phi}-\phi) = 0. \quad (6)$$

Given composite relaxation functions and any loading history, $\sigma^\infty(t)$ with $\lim_{t\to-\infty}\sigma^\infty(t) = 0$, Eq. (6) can be solved numerically for the kink band deformation history, $\phi(t)$. Note that the kink band angle, β, is not determined by this analysis. In fact, β is a required independent variable. Typically, in carbon fiber composites $\beta \approx 20$ deg. Specific forms of the relaxation functions are now considered.

Standard Linear Viscoelastic Model. The standard linear viscoelastic material is sketched in Fig. 2(*a*). The material response satisfies the differential equation

$$\left(1+\frac{k_1}{k_2}\right)\sigma+\frac{\mu}{k_2}\dot{\sigma}=\mu\dot{\epsilon}+k_1\epsilon \tag{7}$$

where σ is stress, ϵ is strain, k_1 and k_2 are elastic moduli, and μ is viscosity. The relaxation function $K(t)$ is defined as the solution, $\sigma(t)$ for an 'input' $\epsilon=H(t)$ where $H(t)$ is the Heaviside step function. Thus, the relaxation function is

$$K(t)=\frac{k_1k_2}{k_1+k_2}\left\{1-\left(1-\frac{k_1+k_2}{k_1}\right)\exp\left[-\frac{t}{\mu}(k_1+k_2)\right]\right\}H(t). \tag{8}$$

Let (G_1,G_2,μ_S) and (E_1,E_2,μ_T) be the material properties (k_1,k_2,μ) for shear and transverse deformation, respectively.

Using Eq. (8), Eq. (6) can be rewritten for the standard linear viscoelastic model. The six dimensional material constants can be reduced to the following four nondimensional constants

$$\lambda\equiv\frac{E_2}{G_2},\ \eta\equiv\frac{\mu_SE_1}{\mu_TG_1},\ \bar{G}\equiv\frac{G_1+G_2}{G_1},\ \bar{E}\equiv\frac{E_1+E_2}{E_1}. \tag{9}$$

With the additional nondimensional substitutions

$$\bar{\sigma}^\infty\equiv\frac{\sigma^\infty}{G_2},\ \bar{t}\equiv\frac{G_1}{\mu_S}t,\ \bar{s}\equiv\frac{G_1}{\mu_S}s, \tag{10}$$

Eq. (6) becomes

$$\bar{\sigma}^\infty[\cos\beta\sin(\bar{\phi}+\phi)+e\cos(\beta+\bar{\phi}+\phi)]$$
$$-\left\{\phi+e\bar{\sigma}^\infty-\int_{-\infty}^{\bar{t}}\bar{K}_S(\bar{t}-\bar{s})[\phi(\bar{s})+e\bar{\sigma}^\infty(\bar{s})]d\bar{s}\right\}\cos(\beta-\bar{\phi}-\phi)$$
$$-\lambda\left\{\phi-\eta\int_{-\infty}^{\bar{t}}\bar{K}_T(\bar{t}-\bar{s})\phi(\bar{s})d\bar{s}\right\}\tan\beta\sin(\beta-\bar{\phi}-\phi)=0 \tag{11}$$

where

$$\bar{K}_S(\bar{t})=(\bar{G}-1)\exp(-\bar{t}\,\bar{G}) \tag{12}$$
$$\bar{K}_T(\bar{t})=(\bar{E}-1)\exp(-\eta\bar{t}\,\bar{E}). \tag{13}$$

Logarithmically Creeping Model. A logarithmically creeping model for composite behavior is proposed based on the results of Horoschenkoff et al. (1988). This material model is shown in Fig. 2(*b*). The response of the system must satisfy

$$\frac{1}{k}\dot{\sigma}+\frac{1}{\mu}\left(\frac{1}{t+t_0}\right)\sigma=\dot{\epsilon} \tag{14}$$

where σ is stress, ϵ is strain, k is an elastic modulus, μ is viscosity, and t_0 is a material time constant. The name for this constitutive law comes from the logarithmic nature of the *creep* function, i.e., the solution $\epsilon(t)$ when $\sigma(t)=H(t)$, given by

$$C(t)=\left[\frac{1}{k}+\frac{1}{\mu}\ln\left(\frac{t}{t_0}+1\right)\right]H(t).$$

The required *relaxation* function is

$$K(t)=k\left(\frac{t}{t_0}+1\right)^{-k/\mu}H(t). \tag{15}$$

Let (G,μ_S,t_{0S}) and (E_T,μ_T,t_{0T}) be the material properties (k,μ,t_0) for shear and transverse deformation, respectively.

For the logarithmically creeping model, the four nondimensional material constants are

$$\lambda\equiv\frac{E_T}{G},\ \eta\equiv\frac{t_{0S}}{t_{0T}},\ \bar{G}\equiv\frac{G}{\mu_S},\ \bar{E}\equiv\frac{E_T}{\mu_T}, \tag{16}$$

and the nondimensional substitutions are

$$\bar{\sigma}^\infty\equiv\frac{\sigma^\infty}{G},\ \bar{t}\equiv\frac{t}{t_{0S}},\ \bar{s}\equiv\frac{s}{t_{0S}}. \tag{17}$$

Rewriting Eq. (6) once again yields (11), but with new kernel functions

$$\bar{K}_S(\bar{t})=\bar{G}(\bar{t}+1)^{-\bar{G}-1} \tag{18}$$
$$\bar{K}_T(\bar{t})=\bar{E}(\eta\bar{t}+1)^{-\bar{E}-1}. \tag{19}$$

Material Properties. Both of the proposed viscoelastic models require four nondimensional material constants. The physical interpretation of these constants is similar for each model. The first constant, λ, is the ratio of the instantaneous transverse stiffness to the instantaneous shear stiffness. Experimental measurements suggest $\lambda=2$ (Hull, 1981). The second material constant, η, is the ratio of viscoelastic time scales in the shear and transverse directions. This ratio is taken to be unity ($\eta=1$) for simplicity. The third and fourth constants, $\bar{G}$ and $\bar{E}$, measure the viscoelastic response in comparison to the initial elastic response for the shear and transverse directions, respectively. Assuming that $\bar{G}=\bar{E}$, what are appropriate ranges of values for analysis? Based on the studies of Ha et al. (1991) and Horoschenkoff et al. (1988), carbon fiber-reinforced epoxy resins are modeled as standard linear viscoelastic materials with a range of $\bar{G}$ of 1.5–10.0 and carbon fiber-reinforced PEEK's are modeled as logarithmically creeping materials with a range of $\bar{G}$ of 0.1–0.4.

Failure Criterion. Failure is associated with debonding of the fiber-matrix interface, matrix microcracking, or with other mechanisms which result in a sharp decrease in the load bearing ability of the kink band. Several failure criteria are possible. It is proposed here that failure occurs when the following simple empirical criterion is satisfied:

$$\left(\frac{e_T}{e_{Tf}}\right)^2+\left(\frac{\gamma}{\gamma_f}\right)^2=1 \tag{20}$$

where e_{Tf} is the transverse failure strain and γ_f is the shear failure strain. It is further assumed that $e_{Tf}\ll\gamma_f$ so that, with Eq. (3),

$$\phi_f\approx\frac{e_{Tf}}{\tan\beta} \tag{21}$$

where ϕ_f is the critical kink band deformation angle at failure. For the purposes of this paper, $e_{Tf}=0.02$. All of these assumptions are in acceptable agreement with experimental evidence (see, for example, Hull, 1981).

A consequence of failure is the concept of failure time or viscoelastic life. Up to this point, only kink band deformation as a function of time, $\phi(t)$, has been discussed. As time, t, tends to infinity, $\phi(t)$ reaches a finite limit in the standard linear viscoelastic model or becomes unbounded in the logarithmically creeping model. Failure occurs at a finite time, t_f, when $\phi=\phi_f$, given by Eq. (21).

Results

Equation (11) is a nonlinear Volterra integral equation of the second kind with well-behaved difference kernels. This equation can be solved numerically by discretizing the integrals using Simpson's rule and stepping forward discretely in time, $t_n=n\Delta t$ where Δt is the step size. At each step, n, a root finding algorithm is used to calculate the deformation angle $\phi_n\equiv\phi(t_n)$ since the discrete solutions from previous steps, ϕ_i $(i=0,1,2,\ldots,n-1)$, are known. It is assumed that the solution is bounded by $0\le\phi<\pi/2$. Techniques for the numerical solution of integral equations can be found in Baker (1977).

Consideration is restricted to loading histories of the form

$$\sigma^\infty(t)=\sigma^\infty H(t) \tag{22}$$

with $e=0$ (i.e., $\tau^\infty=0$). Remote shear stress can be included but does not affect the qualitative features of the results. As previously discussed, $\lambda=2$, $\eta=1$, and $\bar{G}=\bar{E}$. The kink band

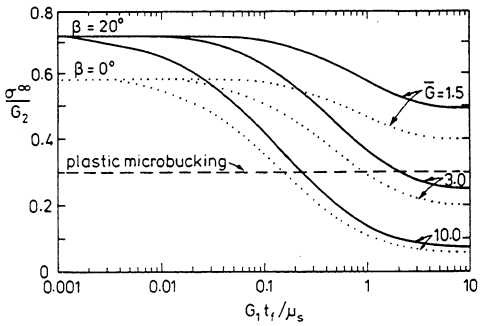

Fig. 3 Applied axial load versus time till failure for the standard linear viscoelastic model ($\lambda = 2$, $\eta = 1$, $\beta = 20$ deg and 0 deg, $\bar{\phi} = 2$ deg, $\phi_f = 3$ deg, $e = 0$, $\bar{E} = \bar{G}$)

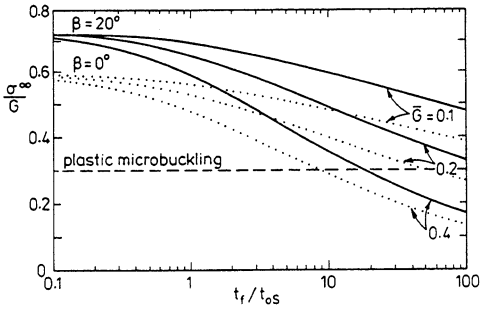

Fig. 5 Applied axial load versus time till failure for the logarithmically creeping model ($\lambda = 2$, $\eta = 1$, $\beta = 20$ deg and 0 deg, $\bar{\phi} = 2$ deg, $\phi_f = 3$ deg, $e = 0$, $\bar{E} = \bar{G}$)

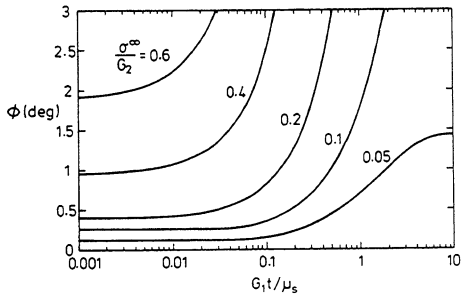

Fig. 4 Kink band deformation angle versus time for the standard linear viscoelastic model ($\lambda = 2$, $\eta = 1$, $\beta = 20$ deg, $\bar{\phi} = 2$ deg, $e = 0$, $\bar{E} = \bar{G} = 10$)

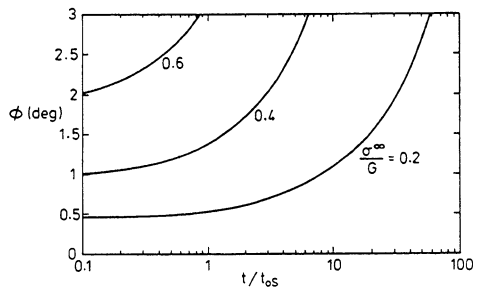

Fig. 6 Kink band deformation angle versus time for the logarithmically creeping model ($\lambda = 2$, $\eta = 1$, $\beta = 20$ deg, $\bar{\phi} = 2$ deg, $e = 0$, $\bar{E} = \bar{G} = 0.4$)

angle is taken to be $\beta = 20$ deg. The critical kink band deformation angle is $\phi_f = 3$ deg via Eq. (21). The case $\beta = 0$ deg is also considered, for comparison, but with $\phi_f = 3$ deg retained. An initial misalignment angle of $\bar{\phi} = 2$ deg is chosen in agreement with measurements on several composites (Budiansky and Fleck, 1993). Results for the standard linear viscoelastic model representing carbon fiber-reinforced epoxy resins are shown in Figs. 3 and 4 and those for the logarithmically creeping model representing carbon fiber-reinforced PEEK's are given in Figs. 5 and 6.

The applied axial stress σ^∞, as defined in Eq. (22), versus the failure time, t_f, is shown in Figs. 3 and 5 for representative $\bar{G}$ values. Experimental results (Ha et al., 1991; Horoschenkoff et al., 1988) indicate timescales t_{0S} and μ_S/G_1 both on the order of one hour. The necessary load for instantaneous failure ($t_f = 0$) is the same for both models and corresponds to the elastic microbuckling load with initial misalignment as calculated by Fleck and Budiansky (1991). The applied axial stress versus failure time for the standard linear viscoelastic model, when plotted on a logarithmic time scale (Fig. 3), has an "S" shaped profile. The applied axial stress versus failure time for the logarithmically creeping model, when plotted on a logarithmic time scale (Fig. 5), is nearly linear over a wide range of failure times. The evolution of kink band deformation, $\phi(t)$, is shown in Figs. 4 and 6 for different loads at a given $\bar{G}$. The ordinate of these plots is terminated at the critical fiber rotation angle $\phi_f = 3$ deg.

For the standard linear viscoelastic model there exists a critical stress, σ^∞_{cr}, below which $\phi(t) < \phi_f$ for all t and failure never occurs. At $\sigma^\infty = \sigma^\infty_{cr}$, $\phi(t \to \infty) = \phi_f$. For small $\bar{\phi}$ and ϕ_f, the critical stress in nondimensional form, $\bar{\sigma}^\infty_{cr} \equiv \sigma^\infty_{cr}/G_2$, follows from Eq. (11) as

$$\bar{\sigma}^\infty_{cr} \approx \left[\frac{1 + \lambda\left(\frac{\bar{G}}{\bar{E}}\right)\tan^2\beta}{(\bar{\phi} + \phi_f) + e\left(1 - \frac{1}{\bar{G}}\right)} \right] \frac{\phi_f}{\bar{G}}. \tag{23}$$

Note from Eq. (23) that $\bar{\sigma}^\infty_{cr}$ decreases linearly with decreasing ϕ_f and decreases with increasing $\bar{G}$. A graphical construction can be used to calculate $\bar{\sigma}^\infty_{cr}$ when $\beta = 0$ deg and $e = 0$ (see Fig. 7). The constitutive Eq. (1) reduces, for small ϕ and $\bar{\phi}$, to

$$\bar{\sigma}^\infty(\bar{\phi} + \phi) \approx \frac{\tau}{G_2}. \tag{24}$$

This equation is represented on the $(\phi, \tau/G_2)$ plane by a line of slope $\bar{\sigma}^\infty$ and intercept $(-\bar{\phi}, 0)$. At $t = 0$, the instantaneous elastic response gives

$$\frac{\tau}{G_2} = \phi \tag{25}$$

which defines a line of slope unity going through the origin on the $(\phi, \tau/G_2)$ plane. At $t \to \infty$, the response is

$$\frac{\tau}{G_2} = \frac{\phi}{\bar{G}} \tag{26}$$

which defines a line of slope $1/\bar{G}$ going through the origin on the $(\phi, \tau/G_2)$ plane. At $t = 0$, the $\tau - \phi$ state of the kink band material is given by the intersection of the lines defined by Eqs. (24) and (25). With increasing time, the $\tau - \phi$ state moves along the ray defined by Eq. (24). For $\bar{\sigma}^\infty$ sufficiently small (e.g., $\bar{\sigma}^\infty_1$ in Fig. 7), $\phi(t \to \infty) < \phi_f$ and failure does not occur; as $t \to \infty$ the $\tau - \phi$ state moves to the intersection of lines defined by Eqs. (24) and (26). At high values of $\bar{\sigma}^\infty$ (e.g., $\bar{\sigma}^\infty_2$ in Fig. 7), ϕ attains ϕ_f at a finite time and failure occurs. At $\bar{\sigma}^\infty = \bar{\sigma}^\infty_{cr}$, ϕ at the intersection of lines (24) and (26) equals ϕ_f.

Discussion

No mention has been made so far of plastic yielding within the kink band. An alternative failure mechanism to viscoelastic microbuckling is plastic instability by plastic microbuckling. A typical critical stress for plastic microbuckling in both PEEK and epoxy systems is $\bar{\sigma}^\infty = 0.3$ (Fleck and Budiansky, 1991). This stress level is shown in Figs. 3 and 5 as a dashed horizontal line. Above this line, failure is due to plastic microbuckling

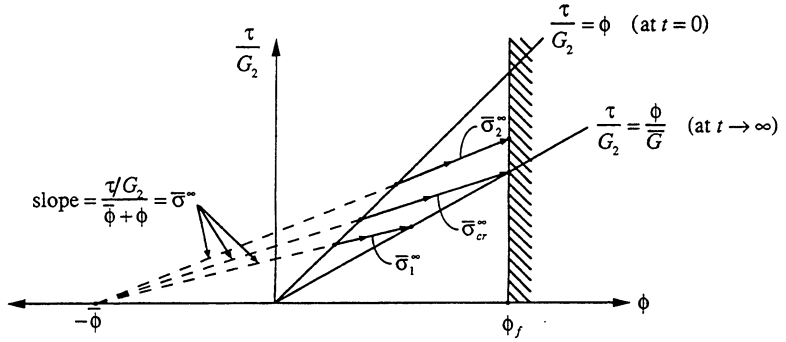

Fig. 7 Stress-strain diagram for the standard linear viscoelastic model when $\beta = 0$ deg and $e = 0$

and failure times from the viscoelastic analysis do not apply. Thus it is seen in Fig. 3 that a carbon fiber-epoxy composite, modeled as a standard linear viscoelastic material, will either fail by plastic microbuckling or not at all if $\bar{G} = 1.5$. For $\bar{G} = 3.0$ and $\bar{G} = 10.0$, viscoelastic microbuckling can occur at stress levels below the plastic microbuckling stress. In order to maximize viscoelastic strength for this material, ϕ_f should be maximized and $\bar{G}$ should be minimized. Figure 5 shows that a carbon fiber-PEEK composite, modeled as a logarithmically creeping solid, fails at low stress levels by viscoelastic microbuckling, for all $\bar{G}$. For example, for $\bar{\sigma}^\infty$, viscoelastic microbuckling requires a minimum of 100 hours ($t_{0S} \approx 1$ hour) at $\bar{G} = 0.2$.

The microbuckling analysis of Budiansky and Fleck (1993), on which this paper is based, follows the collapse response of an imperfect structure. It is not a bifurcation analysis. The effects of fiber bending stiffness are neglected, with the result that there is no length scale in the analysis. Previous studies have shown that this is a valid approximation (Budiansky, 1979). Fibers are implicitly assumed to be broken at the kink band interface, but without fiber bending stiffness this is not an issue. The issue of kink band initiation, in which the kink band might be imagined to begin at some region of local composite weakness or stress concentrator and then propagate out, has not been addressed. This is an important topic and kink bands are seen to form and grow in this way under certain conditions, e.g., at notch tips. However, the nature of the analysis presented here is that the kink band is treated as a one-dimensional structure. No variations in stress or deformation are allowed along the length of the kink band. The relative importance of kink band initiation is a topic for future investigation.

There is a dearth of experimental studies of viscoelastic failure in fiber composites under compression. In part this may be explained by the experimental difficulties that arise from a lack of knowledge of the time scales and loads involved. This situation is aggravated by the inevitable scatter in mechanical properties from one sample to the next. A load that may trigger plastic microbuckling in one sample may be insufficient to cause viscoelastic microbuckling in another. Hopefully, this study will help to alleviate these problems.

Acknowledgments

The authors are grateful for technical discussions with Prof. B. Budiansky. Support from ONR grant 0014-91-J-1916 is gratefully acknowledged.

References

Argon, A. S., 1972, "Fracture of Composites," *Treatise of Materials Science and Technology*, Vol. 1, Academic Press, New York.

Baker, C. H. T., 1977, *The Numerical Treatment of Integral Equations*, Oxford University Press, Oxford, U.K.

Budiansky, B., 1979, "Remarks on Kink Formation in Axially Compressed Fiber Bundles," Preliminary Reports, Memoranda and Technical Notes of the Materials Research Council Summer Conference, La Jolla, CA, July 1979, sponsored by DARPA.

Budiansky, B., and Fleck, N. A., 1993, "Compressive Failure of Fiber Composites," *J. Mech. Phys. Solids*, Vol. 41, No. 8, pp. 1265–1284.

Dinwoodie, J. M., 1981, *Timber: Its Nature and Behavior*, Van Nostrand Reinhold Company, Berkshire, U.K.

Fleck, N. A., and Budiansky, B., 1991, "Compressive Failure of Fiber Composites Due to Microbuckling," *Proc. IUTAM Symp. on Inelastic Deformation of Composite Materials*, J. Dvorak, ed., Troy, NY, May 29–June 1, 1990, Springer-Verlag, New York, pp. 235–273.

Grossman, P. U. A., and Wold, M. B., 1971, "Compressive Fracture of Wood Parallel to the Grain," *Wood Sci. Tech.*, Vol. 5, pp. 147–156.

Ha, S. K., Wang, Q., and Chang, F., 1991, "Modeling the Viscoplastic Behavior of Fiber-Reinforced Thermoplastic Matrix Composites at Elevated Temperatures," *J. Comp. Mat.*, Vol. 25, pp. 335–373.

Horoschenkoff, A., Brandt, J., Warnecke, J., and Brüller, O. S., 1988, "Creep Behavior of Carbon Fiber Reinforced Polyetheretherketone and Epoxy Resin," *New Generation Materials and Processes*, Milan.

Hull, D., 1981, *An Introduction to Composite Materials*, Cambridge University Press, Cambridge, U.K.

Mark, R. E., 1967, *Cell Wall Mechanics of Tracheids*, Yale University Press, New Haven, CT.

Rosen, B. W., 1965, "Mechanics of Composite Strengthening," *Fiber Composite Materials, Am. Soc. Metals Seminar*, Chapter 3.

Soutis, C., 1991, "Measurements of the Static Compressive Strength of Carbon Fiber-Epoxy Laminates," *Comp. Sci. Tech.*, Vol. 42, No. 4, pp. 373–392.

Steif, P. S., 1988, "A Simple Model for the Compressive Failure of Weakly Bonded, Fiber-Reinforced Composites," *J. Comp. Mat.*, Vol. 22, pp. 818–828.